Tris(2-methoxyphenyl) phosphite complexes of platinum(II): the *cis* preference of triaryl phosphite ligands and the effect of oxidation state on metal–phosphite bonding †

Alessandra Crispini, Karl N. Harrison, A. Guy Orpen,* Paul G. Pringle * and James R. Wheatcroft

School of Chemistry, University of Bristol, Cantocks Close, Bristol BS8 1TS, UK

The complexes *cis*-[PtX$_2$\{P(OC$_6$H$_4$OMe-2)$_3$\}$_2$] (X = Cl, Br or I) have been prepared by treatment of the corresponding [PtX$_2$(cod)] (cod = cycloocta-1,5-diene) with P(OC$_6$H$_4$OMe-2)$_3$. That with X = Cl reacted with 1 or 2 equivalents of SnCl$_2$ to give *cis*-[PtCl(SnCl$_3$)\{P(OC$_6$H$_4$OMe-2)$_3$\}$_2$] or *trans*-[Pt(SnCl$_3$)$_2$\{P(OC$_6$H$_4$OMe-2)$_3$\}$_2$]. The unstable hydride *trans*-[PtH(Cl)\{P(OC$_6$H$_4$OMe-2)$_3$\}$_2$] was detected when *cis*-[PtCl$_2$\{P(OC$_6$H$_4$OMe-2)$_3$\}$_2$] was treated with NaBH$_4$ or [Pt\{P(OC$_6$H$_4$OMe-2)$_3$\}$_3$] with HCl. The organoplatinum complexes *cis*-[PtR$_2$\{P(OC$_6$H$_4$OMe-2)$_3$\}$_2$] and *cis*-[PtR(X)\{P(OC$_6$H$_4$OMe-2)$_3$\}$_2$] (R = Me, X = Cl, I or CN; R = Et, X = Cl) were obtained from platinum-(II) and -(0) precursors. Addition of HBF$_4$ to *cis*-[PtMe$_2$\{P(OC$_6$H$_4$OMe-2)$_3$\}$_2$], in the presence of H$_2$O or MeCN, gave the cationic species *cis*-[PtMe(L)\{P(OC$_6$H$_4$OMe-2)$_3$\}$_2$][BF$_4$] (L = H$_2$O or MeCN). The significance of the observation that complexes of the type [PtMe(L)\{P(OC$_6$H$_4$OMe-2)$_3$\}$_2$] are invariably *cis* is discussed. The crystal structures of *cis*-[PtCl$_2$\{P(OC$_6$H$_4$OMe-2)$_3$\}$_2$] and *cis*-[PtMe(OH$_2$)\{P(OC$_6$H$_4$OMe-2)$_3$\}$_2$][BF$_4$]·CH$_2$Cl$_2$ have been determined. These, together with those previously reported for P(OC$_6$H$_4$OMe-2)$_3$ and [Pt(η-C$_2$H$_4$)-\{P(OC$_6$H$_4$OMe-2)$_3$\}$_2$], show pronounced variation in P–O lengths and O–P–O bond angles consistent with the greater importance of Pt–P π bonding in the platinum(0) species. The phosphite P(OC$_6$H$_4$OMe-2)$_3$ shows a range of conformations in the structures and that with *anti, gauche, gauche* (*agg*) conformation about the P–O bonds apparently favoured in general but *ggg* attainable in the absence of steric crowding. In *cis*-[PtMe(OH$_2$)\{P(OC$_6$H$_4$OMe-2)$_3$\}$_2$][BF$_4$]·CH$_2$Cl$_2$, intramolecular hydrogen bonding leads to an unusual *aag* conformation. Weak Pt · · · O interactions involving the OMe groups of the phosphite ligand are observed in these structures. The correlation of P–O length and O–P–O angle variation is mirrored by similar behaviour for 133 Z–P(OPh)$_3$ (Z = O, N or metal) structures. These observations are consistent with the now conventional view of M–P π bonding.

Nickel(0) phosphite-catalysed hydrocyanation is one of the most important applications of transition-metal homogeneous catalysis.[1] The recent exciting developments in rhodium phosphite-catalysed hydroformylation[2] may partly explain the upsurge of interest in phosphite ligands.[3] However, the systematic study of metal phosphite complexes is a poorly developed area of academic endeavour compared to the enormous effort that has been expended in fine-tuning metal phosphines.[4] We are interested in fundamental studies on phosphite co-ordination chemistry and on the rational design of new phosphites for catalysis.[4,5] Tris(2-methoxyphenyl) phosphite **I** is a functionalised phosphite which has the potential to form hemilabile chelates in a similar manner to that of phosphinoethers.[6] We have previously shown[4] that in the co-ordination chemistry of **I** with platinum(0) and nickel(0) the effect of the methoxy group was largely a passive, steric one. In this paper, the chemistry of platinum(II) complexes of the type [PtX$_2$\{P(OC$_6$H$_4$OMe-2)$_3$\}$_2$] (X = Cl, Br, I or Me) is described and it is shown that in these systems the ether donor can play a more active role. Observations are made on the tendency of phosphite ligands to be *cis* in platinum(II) complexes and changes in the metrical parameters for co-ordinated phosphite ligands are correlated with the M–P bonding.

Only a few previous reports of the chemistry and catalytic properties of complexes of the type [PtX$_2$\{P(OR)$_3$\}$_2$] (R = aryl) have been made.[7–9] In 1973 Robinson and co-workers[7]

reported an extensive study of the complexes [PtX$_2$\{P(OR)$_3$\}$_2$] (X = Cl, Br or I, R = substituted phenyl) and more recently the mixed [PtX$_2$\{P(OR)$_3$\}$_2$]–SnCl$_2$ systems have been investigated as catalysts for hydrogenation and hydroformylation.[8]

Results and Discussion

Synthesis and characterisation of the complexes

The synthetic chemistry is summarised in Schemes 1 and 2. Treatment of [PtCl$_2$(cod)] (cod = cycloocta-1,5-diene) with **I** gave complex **2a** plus a minor (*ca.* 5%) amount of a transient species observed only in reaction mixtures and assigned to *trans*-[PtCl$_2$\{P(OC$_6$H$_4$OMe-2)$_3$\}$_2$] **2** on the basis of its ^{31}P NMR parameters being similar to the literature values for *trans*-[PtCl$_2$\{P(OPh)$_3$\}$_2$].[7] Complex **1a** has been fully characterised (see Tables 1 and 2) and its crystal structure determined (see below). The bromo (**1b**) and iodo (**1c**) complexes were made either by treatment of [PtX$_2$(cod)] (X = Br or I) with **I**, or by metathesis of the chlorides in **1a** using LiBr or LiI. The mono- and bis-trichlorotin species **3** and **4** were made by addition of the appropriate amount of SnCl$_2$ to **1a**; the ^{31}P NMR data for **3** and **4** are similar to those reported for the P(OPh)$_3$ analogues.[8]

The hydrido complex *trans*-[PtH(Cl)\{P(OC$_6$H$_4$OMe-2)$_3$\}$_2$] **5** has been identified from ^{1}H and ^{31}P NMR spectroscopy as the product of addition of NaBH$_4$ to **1a** in MeCN. The same species is also observed upon addition of HCl to the platinum(0) complex [Pt\{P(OC$_6$H$_4$OMe-2)$_3$\}$_3$]. It has been characterised only in solution because it decomposes over a few hours at ambient temperatures to a mixture of products, one of which was identified as the platinum(0) complex [Pt\{P(OC$_6$H$_4$OMe-
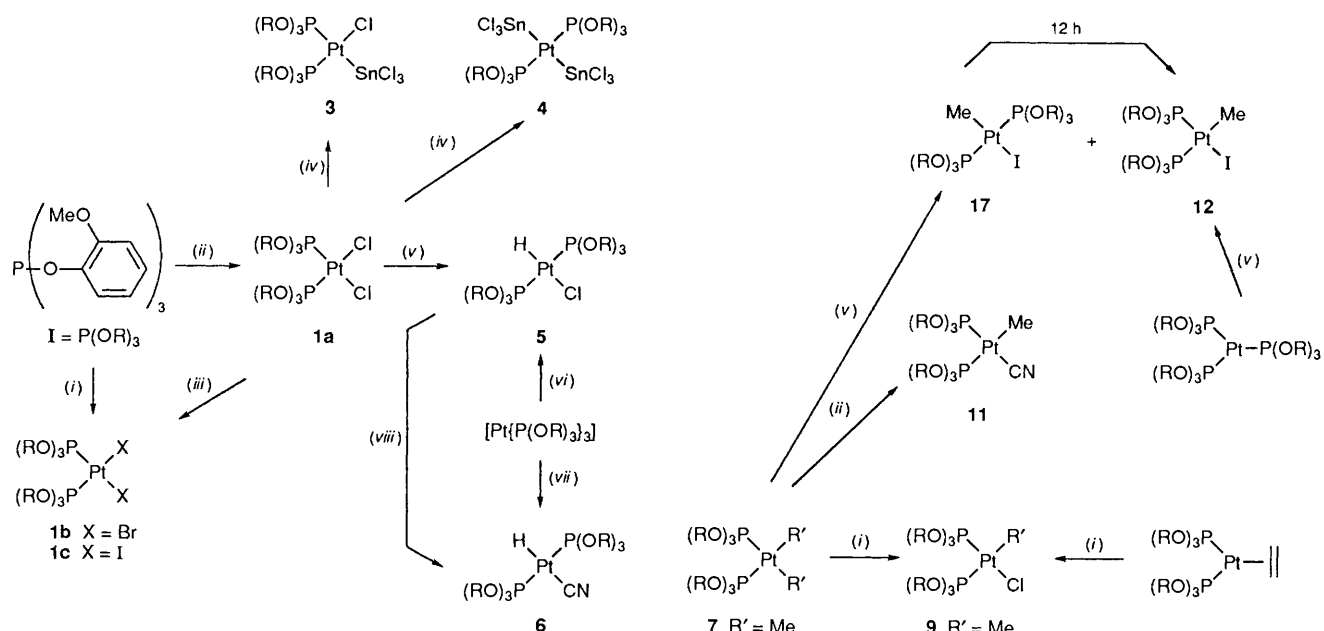
Scheme 1 (i) [PtX₂(cod)]; (ii) [PtCl₂(cod)]; (iii) LiX; (iv) SnCl₂; (v) NaBH₄; (vi) HCl; (vii) Me₂CO·HCN; (viii) NaCN

I = P(OR)₃

1a   1b X = Br   1c X = I   3   4   5   6

2)₃}₃].⁴ The phosphite complex *trans*-[PtH(Cl){P(OMe)}₂] is reported¹⁰ to be even less stable than 5, decomposing above −40 °C. A hydrido species that was stable in MeCN solution for days was obtained upon addition of NaCN to 5 or upon treatment of [Pt{P(OC₆H₄OMe-2)₃}₃] with Me₂CO·HCN. This new species was assigned to the cyano derivative *trans*-[PtH(CN){P(OC₆H₄OMe-2)₃}₂] 6 on the basis of its ¹H and ³¹P NMR spectra (Table 2) but was not further characterised.

The alkylplatinum(II) chemistry of complexes of I is summarised in Scheme 2. The dimethyl complex 7 is made by substitution of cod from [PtMe₂(cod)] and the diethyl complex 8 is made by treatment of 1a with AlEt₃. Addition of HCl to 7 or 8 gave the corresponding chloro complex 9 or 10. When 7 was treated with Me₂CO·HCN, after 24 h, a new species was assigned from its ³¹P NMR spectrum to *cis*-[PtMe(CN)-{P(OC₆H₄OMe-2)₃}₂] 11. This product was not isolated because, under these conditions, the reaction was only 10% complete and if the reaction mixture was heated, decomposition occurred. An alternative entry into the alkylplatinum(II) chemistry of I is via its platinum(0) complexes⁴ (see Scheme 2). Thus addition of MeI to [Pt{P(OC₆H₄OMe-2)₃}₃] gave 12 and addition of HCl to [Pt(C₂H₄){P(OC₆H₄OMe-2)₃}₂] gave 10.

Treatment of the dimethyl complex 7 with HBF₄ in the presence of water or MeCN gave the solvento complexes 13 and 14 as shown by their characteristic ³¹P NMR spectra (Table 2). The crystal structure of 13 (see below) revealed the presence of an intramolecular hydrogen bond between a co-ordinated water and one of the *o*-OMe groups. This may explain why the ³¹P NMR parameters for the deuteriated analogue 13d are significantly different from those of 13 (see Table 2), particularly for the phosphite *trans* to the aqua ligand.

We have previously shown¹¹ that protonation of dimethyl-platinum(II) complexes with HBF₄ in Et₂O is a convenient route to hemilabile chelates of platinum(II). Thus, in an attempt to promote co-ordination of the methoxy group, the dimethyl complex 7 was treated with 1 equivalent of HBF₄ in Et₂O. A mixture of three species A–C in the ratio 1:2:2 was obtained, as shown by ³¹P NMR spectroscopy at −80 °C. Three AB patterns were observed each of which had parameters characteristic of a complex of the type *cis*-[PtMe-(L){P(OC₆H₄OMe-2)₃}₂]; in particular, each had one small ¹J(PtP) for a P(OR)₃ *trans* to a Me, one large ¹J(PtP) for a P(OR)₃ *trans* to a weak σ donor, and a small ²J(PP) typical of a
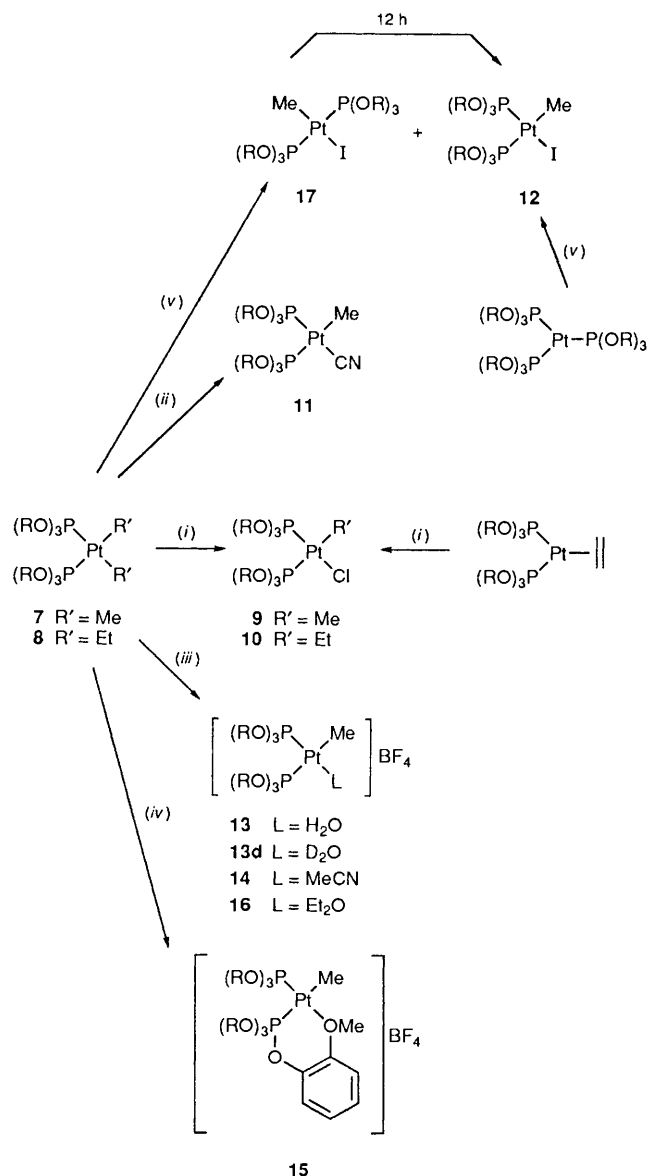
Scheme 2 R = 2-MeOC₆H₄. (i) HCl; (ii) Me₂CO·HCN; (iii) HBF₄, L; (iv) HBF₄; (v) MeI

7 R' = Me   8 R' = Et   9 R' = Me   10 R' = Et
11   12   17

13 L = H₂O   13d L = D₂O   14 L = MeCN   16 L = Et₂O
15

Table 1 Elemental analyses (calculated values in parentheses)

Complex	C	H
1a	46.9 (47.3)	3.9 (4.0)
1b	43.2 (43.7)	3.8 (3.7)
1c *	39.4 (39.4)	3.3 (3.4)
3	40.5 (40.2)	3.1 (3.4)
4	35.2 (34.9)	3.0 (2.9)
7	51.0 (51.5)	4.8 (4.7)
8	51.1 (50.9)	5.0 (4.8)
9a	49.4 (49.4)	4.4 (4.3)
10	48.1 (48.4)	4.5 (4.4)

* Contains 0.5 equivalent of CH₂Cl₂.

cis disposition of the P nuclei (see Experimental section for the data). At +20 °C two broad signals were observed, envelopes of the two groups of doublets at −80 °C, indicating that interconversion takes place among A–C. One of these species (A) has δ(P) for the P *trans* to Me some 20 ppm to high frequency of B and C and is tentatively assigned to the chelate 15. Species B was identified as the water complex 13 (from adventitious water) and C is tentatively assigned to the Et₂O

Table 2 Phosphorus-31 [a] and ^{195}Pt [b] NMR data

Complex	δ(P$_A$)	^1J(PtP$_A$)	δ(P$_B$)	^1J(PtP$_B$)	^2J(P$_A$P$_B$)	δ(Pt)
1a	58.5	5918				−224.6
1b	59.2	5889				−42.5
1c	60.5	5694				−621.8
2	75.1	4507				
3	79.0	5031	69.5	6068	26	−61.1
4	89.4	4223				−712.7 [c]
5 [d]	91.2	5186				
6 [e]	111.7	4971				
7	121.9	3086				−37.8
8	122.8	2813				−114.9
9	122.7	2842	78.4	7089	33	30.8
10	79.9	2545	125.3	7634	37	−6.6
11	120.4	2968	71.1	6781	33	
12	117.7	2845	99.1	5066	40	
13	130.2	2988	59.6	8204	39	
13d	130.2	3033	63.9	8061	35	
14	121.5	3064	66.0	7642	39	84.2
17	98.9	5238				

[a] Spectra (36.2 or 161 MHz) measured in CDCl$_3$ at 28 °C unless otherwise stated. Chemical shifts (δ) in ppm (± 0.1) to high frequency of 85% H$_3$PO$_4$. Coupling constants (J) in Hz (± 3). [b] Spectra (19.2 or 107.0 MHz) measured at 28 °C in CDCl$_3$ unless stated otherwise. Chemical shifts (δ) in ppm (± 0.5) to high frequency of Ξ(Pt) = 21.4 MHz. Coupling constants (J) in Hz (± 10). [c] ^1J(PtSn) 10 213, ^2J(PSn) 272 Hz. [d] δ(H) − 16.43, ^1J(PtH) 1123, ^2J(PH) 7 Hz. [e] δ(H) − 8.45, ^2J(PH) 7 Hz, ^1J(PtH) not resolved.

complex **16** in which the ether ligand derives from that in the HBF$_4$ reagent.

cis Preference of phosphite ligands

The compound **I** and P(OPh)$_3$ have a tendency to form cis complexes with platinum(II).[12] This is particularly apparent for the [PtMe(X){P(OC$_6$H$_4$OMe-2)$_3$}$_2$] systems (X = Cl, I, CN, H$_2$O or MeCN) which are all exclusively cis. Addition of MeI to [Pt{P(OC$_6$H$_4$OMe-2)$_3$}$_3$] or [PtMe$_2${P(OC$_6$H$_4$OMe-2)$_3$}$_2$] initially gave mixtures of cis and trans isomers of [PtMe(I){P(OC$_6$H$_4$OMe-2)$_3$}$_2$] (**12** and **17**) but over a period of 12 h these mixtures isomerised to give exclusively the cis isomer **12**, which shows that it is the thermodynamic product.

For phosphine complexes of the type [PtR(L)(PR$_3$)$_2$] (R = H or Me; L = halide or solvent) the trans isomers are known generally to be more stable than the cis and it has been suggested [13] that this can be partly explained by the fact that the bonding of the strong σ donors (H and Me) is maximised when they are trans to the weaker σ donor, e.g. Cl rather than PR$_3$. Phosphites are poorer σ donors than phosphines and therefore this aspect of the stabilisation of the trans isomer will be less important for the phosphite analogues [PtMe(L){P(OR)$_3$}$_2$]. In contrast M–P π back bonding, which is more important for phosphites than phosphines,[14] would favour a cis-phosphorus disposition in which all the d$_π$ orbitals can interact with the phosphorus π-acceptor orbitals. Finally phosphite ligands are likely to be more flexible, in terms of the variation of conformation (about the P–O, cf. P–C bonds) than are phosphines, and as a consequence seem likely to suffer less serious steric crowding when mutually cis.

The tendency of phosphites to favour a cis disposition of the ligands opposite them should lead to the promotion of ligand interactions such as reductive eliminations. This may explain why {unlike the phosphine complexes trans-[PtH(Cl)(PR$_3$)$_2$]} the phosphite complexes trans-[PtH(Cl){P(OR)$_3$}$_2$] are kinetically unstable [10] with respect to platinum(0) (see above): the reductive elimination of HCl from the phosphite complexes would be facilitated by transient formation of a phosphite-stabilised cis-[PtH(Cl){P(OR)$_3$}$_2$]. If the cis preference of phosphites is general for d^8 systems, it may be one of the features that make metal phosphite complexes such good homogeneous catalysts; for example, the rate-determining step in nickel phosphite-catalysed hydrocyanation is reductive elimination of RCN.[15]
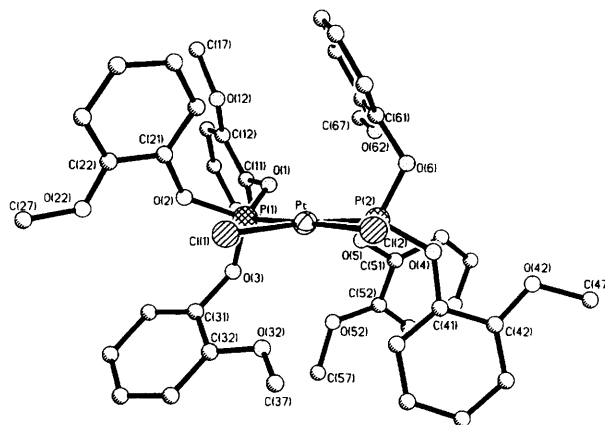

Fig. 1 Molecular structure of cis-[PtCl$_2${P(OC$_6$H$_4$OMe-2)$_3$}$_2$] **1a** showing the atom labelling. All hydrogen atoms have been omitted for clarity

Structural studies

Crystal structure analyses of complexes **1a** and **13·CH$_2$Cl$_2$** revealed the molecular structures shown in the schemes. In particular the cis disposition of the P(OC$_6$H$_4$OMe-2)$_3$ ligands in both structures is confirmed. Figs. 1 and 2 show the molecular structures and Tables 3 and 4 list selected bond distances and angles for **1a** and **13**. In each case the co-ordination environment at platinum is planar, as expected for Pt^{II}, with only minor deviations from the mean plane through Pt and the four contact atoms [root mean square (r.m.s) deviations of 0.032 and 0.044 Å for **1a** and **13·CH$_2$Cl$_2$**, respectively]. The angular distortions from ideal values of 90 and 180° are not large, the most notable being the cis P–Pt–P angles which are ca. 95°. The Pt–P bond lengths are similar to those in a range of triphenyl phosphite platinum complexes (which average 2.226 Å with sample standard deviation 0.032 Å, see below for a more general survey). The individual Pt–P distances reflect the variations in trans influence of the ligands trans to the P(OC$_6$H$_4$OMe-2)$_3$. Thus the shortest Pt–P bond [2.131(6) Å] lies trans to the aqua ligand in **13**, the longest [2.273(5) Å] lies trans to the methyl ligand also in **13**, with intermediate lengths for the Pt–P bond trans to chlorine [2.199(2) and 2.207(2) Å] in **1a**. These Pt–P distances correlate reasonably well with the

Table 3 Selected bond lengths (Å) and angles (°) for complex **1a**

Pt–Cl(1)	2.343(2)	O(62)–C(67)	1.458(10)	O(4)–C(41)	1.396(11)	P(2)–O(5)	1.585(6)
Pt–P(2)	2.207(2)	O(12)–C(17)	1.456(11)	O(5)–C(51)	1.387(10)	C(32)–O(32)	1.358(9)
P(1)–O(2)	1.580(5)	O(22)–C(27)	1.441(12)	O(6)–C(61)	1.401(10)	C(42)–O(42)	1.355(10)
P(2)–O(6)	1.588(5)	Pt–Cl(2)	2.346(2)	O(1)–C(11)	1.419(9)	C(52)–O(52)	1.342(10)
O(32)–C(37)	1.433(9)	P(1)–O(3)	1.577(5)	O(2)–C(21)	1.400(10)	C(62)–O(62)	1.353(11)
O(42)–C(47)	1.459(10)	P(2)–O(4)	1.587(6)	Pt–P(1)	2.199(2)	C(12)–O(12)	1.370(11)
O(52)–C(57)	1.454(10)	O(3)–C(31)	1.416(8)	P(1)–O(1)	1.576(5)	C(22)–O(22)	1.351(11)
Cl(1)–Pt–Cl(2)	89.1(1)	Cl(1)–Pt–P(1)	88.9(1)	O(4)–P(2)–O(6)	95.3(3)	O(5)–P(2)–O(6)	108.0(3)
Cl(2)–Pt–P(1)	177.8(1)	Cl(1)–Pt–P(2)	174.8(1)	P(1)–O(3)–C(31)	125.7(5)	C(32)–O(32)–C(37)	117.9(5)
Cl(2)–Pt–P(2)	87.5(1)	P(1)–Pt–P(2)	94.5(1)	P(2)–O(4)–C(41)	124.7(5)	C(42)–O(42)–C(47)	116.9(7)
Pt–P(1)–O(3)	116.1(2)	Pt–P(1)–O(1)	110.8(2)	P(2)–O(5)–C(51)	126.5(5)	C(52)–O(52)–C(57)	118.5(7)
O(3)–P(1)–O(1)	102.0(3)	Pt–P(1)–O(2)	120.1(2)	P(2)–O(6)–C(61)	121.2(4)	C(62)–O(62)–C(67)	118.7(7)
O(3)–P(1)–O(2)	100.2(3)	O(1)–P(1)–O(2)	105.6(3)	P(1)–O(1)–C(11)	126.0(4)	C(12)–O(12)–C(17)	117.3(7)
Pt–P(2)–O(4)	117.8(2)	Pt–P(2)–O(5)	112.6(2)	P(1)–O(2)–C(21)	128.4(4)	C(22)–O(22)–C(27)	117.8(7)
O(4)–P(2)–O(5)	104.9(3)	Pt–P(2)–O(6)	116.5(2)				

Table 4 Selected bond lengths (Å) and angles (°) for complex **13·CH₂Cl₂**

Pt–P(1)	2.273(5)	C(32)–C(37)	1.403(39)	O(4)–C(41)	1.388(24)	P(2)–O(5)	1.574(15)
Pt–C(2)	2.058(19)	C(52)–O(52)	1.377(29)	C(12)–O(12)	1.318(25)	O(2)–C(21)	1.371(23)
P(1)–O(3)	1.589(14)	O(62)–C(67)	1.440(26)	O(22)–C(27)	1.467(34)	O(5)–C(51)	1.410(26)
P(2)–O(6)	1.565(14)	Pt–P(2)	2.131(6)	C(42)–O(42)	1.359(24)	O(12)–C(17)	1.466(41)
O(3)–C(31)	1.414(23)	P(1)–O(1)	1.585(15)	O(52)–C(57)	1.416(28)	C(32)–O(32)	1.380(28)
O(6)–C(61)	1.399(26)	P(2)–O(4)	1.594(10)	Pt–O(7)	2.079(15)	O(42)–C(47)	1.426(35)
C(22)–O(22)	1.359(28)	O(1)–C(11)	1.446(22)	P(1)–O(2)	1.566(12)	C(62)–O(62)	1.390(24)
P(1)–Pt–P(2)	95.8(2)	P(1)–Pt–O(7)	90.8(4)	O(4)–P(2)–O(6)	97.9(7)	O(5)–P(2)–O(6)	102.4(8)
P(2)–Pt–O(7)	171.4(4)	P(1)–Pt–C(2)	174.3(6)	P(1)–O(1)–C(11)	124.9(12)	P(1)–O(2)–C(21)	132.1(13)
P(2)–Pt–C(2)	89.9(6)	O(7)–Pt–C(2)	83.4(7)	P(1)–O(3)–C(31)	126.8(13)	P(2)–O(4)–C(41)	124.9(11)
Pt–P(1)–O(2)	111.7(5)	Pt–P(1)–O(2)	112.9(6)	P(2)–O(5)–C(51)	128.5(11)	P(2)–O(6)–C(61)	121.6(15)
O(1)–P(1)–O(2)	102.6(7)	Pt–P(1)–O(3)	120.9(5)	C(12)–O(12)–C(17)	116.4(22)	C(22)–O(22)–C(27)	115.9(16)
O(1)–P(1)–O(3)	104.7(8)	O(2)–P(1)–O(3)	102.1(5)	C(32)–O(32)–C(37)	116.6(16)	C(42)–O(42)–C(47)	115.5(20)
Pt–P(2)–O(4)	120.6(6)	Pt–P(2)–O(5)	113.2(5)	C(52)–O(52)–C(57)	117.9(21)	C(62)–O(62)–C(67)	112.5(19)
O(4)–P(2)–O(5)	103.9(7)	Pt–P(2)–O(6)	116.3(6)				

Table 5 Torsion angles (°) M–P–O–C and P–O–C–C(OMe) in P(OC₆H₄OMe-2)₃ moieties[a]

Compound	M–P–O–C	Conformation types[b]	P–O–C–C(OMe)	Conformation types	Maximum cone angle, θ
I P(OC₆H₄OMe-2)₃ (L)	31, 31, 31[c]	g, g, g	−123, −123, −123	a, a, a	180.6
[Pt(η²-C₂H₄)L₂]	−172, 61, 7	a, g, g	133, 128, −116	a, a, a	196.8
	−45, −41, −35	g, g, g	148, 99, 154	a, a, a	214.2·
1a [PtCl₂L₂]	172, 36, 82	a, g, g	105, −146, −81	a, a, g	246.8
	−154, 77, −40	a, g, g	155, 130, −95	a, a, a	197.8
13 [PtMe(OH₂)L₂]⁺	−174, −122, 11	a, a, g	−93, 126, 55	a, a, g	219.2
	32, 169, 46	a, g, g	133, 107, 91	a, a, a	234.6

[a] The (O)C–C–O–Me torsion angle magnitudes lie in the range 151–180°. [b] a = anti, torsion angle magnitude >90°; g = gauche, torsion angle magnitude <90°. [c] Angles calculated relative to a dummy metal atom placed on the molecular C_3 axis.

observed ^1J(Pt–P) values (8204 and 2988 for **13** and 5918 Hz for **1a**). The Pt–Cl distances in **1a** [2.343(2) and 2.346(2) Å] are very similar to that *trans* to P(OPh)₃ in cis-[PtCl₂(PEt₃){P(OPh)₃}] (2.344 Å).[16]

The o-OMe groups of the phosphite ligands are involved in weak contacts with the platinum(II) centres in both **1a** and **13**. Thus the Pt ··· O(32) distance in **1a** is 3.216(5) Å, while in **13** there are two such contacts [Pt ··· O(32) 3.33(1) and Pt ··· O(62) 3.38(1) Å]. These lie well out of the platinum co-ordination plane (at angles of 70.1, 48.2 and 73.7° to the plane respectively). In contrast there are no such contacts shorter than 3.75 Å in the structure of [Pt(η²-C₂H₄){P(OC₆H₄OMe-2)₃}₂].[4] It seems likely that these contacts will be strongest when the metal centre carries a high positive charge.

The P(OC₆H₄OMe-2)₃ ligands are flexible by torsion about the P–O and O–C$_{ipso}$ bonds and adopt a variety of conformations in **I**,[4] **1a**, **13** and [Pt(η²-C₂H₄){P(OC₆H₄OMe-2)₃}₂],[4] as is reflected in the torsion-angle data given in Table 5. In contrast, the C$_{ipso}$–C–O–Me torsion angles are all close to the ideal *anti* value of 180°, as would be expected.[17] The variation

in M–P–O–C and P–O–C–C(OMe) torsion angles leads to a spread of cone angles (176–247°) as calculated from the crystal structures. If the phosphite ligand P(1) in complex **13** is excluded (see below), the M–P–O–C torsion angle magnitudes fall into two groups: *gauche*, with values between 7 and 82° and *anti*, with values between 154 and 174°. In contrast the P–O–C–C(OMe) torsion angle magnitudes fall in one range from 81 and 155°, all but one above 90°, without clearly defined subdivisions. The triplets of M–P–O–C torsion angles are all either *anti, gauche, gauche (agg)* (as in all but one of the phosphite ligands in this paper) or *gauche, gauche, gauche (ggg)* (as in free **I** and one of the phosphite ligands of the relatively uncrowded [Pt(η²-C₂H₄){P(OC₆H₄OMe-2)₃}₂]). The unusual M–P–O–C torsion angle set is that of P(1) in **13** in which one methoxy oxygen is involved in an intramolecular hydrogen bond with the aqua oxygen [O(7) ··· O(32) 2.77(2) Å]. The ring-closure constraints of this hydrogen bond are presumably responsible for the atypical M–P–O–C torsion angle (−122°) for the aryl group containing O(32) and the unique *aag* conformation of the ligand involved. The strong inclination of

**Table 6** Mean bond lengths (Å) and angles (°) in $P(OC_6H_4OMe-2)_3$ moieties

Compound	Oxidation state	Pt–P	Mean P–O, d	Mean O–P–O, α
I $P(OC_6H_4OMe-2)_3$ (L)	—	—	1.624(2)	96.6(1)
$[Pt(\eta^2-C_2H_4)L_2]$	Pt^0	2.228	1.615(7)	99.6(9)
		2.227	1.620(3)	96.8(9)
1a $[PtCl_2L_2]$	Pt^{II}	2.200	1.582(1)	102.7(12)
		2.207	1.585(1)	102.7(30)
13 $[PtMe(OH_2)L_2]^+$	Pt^{II}	2.273	1.580(6)	103.1(6)
		2.131	1.578(7)	101.4(14)
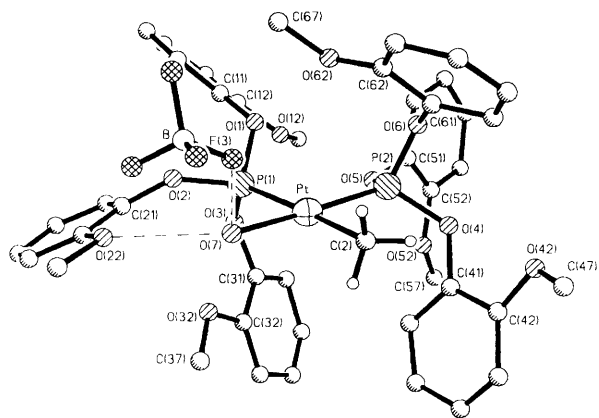
Fig. 2 Molecular structure of the cation of cis-[PtMe-$(OH_2)\{P(OC_6H_4OMe-2)_3\}_2][BF_4]$ **13** showing the atom labelling. All hydrogen atoms have been omitted for clarity. The intramolecular hydrogen bonds between the aqua ligand and the BF_4^- anion and one o-methoxy group are shown as dashed lines

Fig. 3 Scattergram of mean P–O $(d/Å)$ and O–P–O $(\alpha/°)$ values for 133 $Z-P(OPh)_3$ [Z = O (Δ), N (Δ) or M(+)] fragments retrieved from the CSD

the aqua ligand to hydrogen bond is further indicated by its short intermolecular hydrogen-bonding contact with the BF_4^- anion, a very weak Lewis base, in **13** [O(7) ··· F(3) 2.62(2) Å].

The $P(OC_6H_4OMe-2)_3$ ligands display some variation of geometry in the series of structures determined to date (i.e. of **I**, $[Pt(\eta^2-C_2H_4)\{P(OC_6H_4OMe-2)_3\}_2]$, **1a** and **13**). Thus the average P–O distances (d) vary from 1.578 to 1.624 Å and mean O–P–O angles (α) vary from 96.6 to 103.1° (see Table 6). The correlation of d and α is notable (correlation coefficient 0.88) and similar to that determined in our study of $Z-PPh_3$ species $(Z = C, O, S$, transition metals, etc.)[18] in which mean P–C and C–P–C angles were also observed to be negatively correlated. This correlation was interpreted in terms of a molecular orbital model of phosphine–metal (or other substrate) bonding which predicts that d will increase and α decrease (or vice versa) in sympathy. In this model, increased σ donation leads to low d and high α and increased π back donation to the phosphorus ligand leads to larger d and reduced α. The values of d and α for **I** seem to depend on the oxidation state of the platinum: the platinum(II) complexes **1a** and **13** show low d and high α as would be expected for reduced π back bonding and strong σ donation, while the platinum(0) complex $[Pt(\eta^2-C_2H_4)-\{P(OC_6H_4OMe-2)_3\}_2]$ shows larger d and lower α as would be expected for more π back bonding and/or less σ donation. Free **I** has d and α values close to those of the platinum(0) complex.

In order to test the generality of these observations we have surveyed the $Z-P(OPh)_3$ complexes $(Z =$ any atom) the structures of which are recorded in the Cambridge Structural Database (CSD).[19] There are 84 such structures {of reasonable precision (crystallographic $R < 0.07$) and not suffering from disorder} in the April 1995 version of the CSD which contains 140 268 structures in total. The 133 unique $Z-P(OPh)_3$ fragments present in these crystal structures show negative correlation between d and α values (see Fig. 3, tabulated values
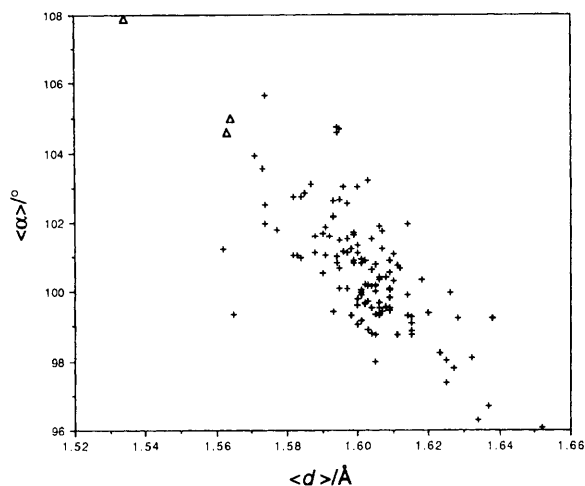
have been deposited as SUP 57119) similar to those observed for the $P(OC_6H_4OMe-2)_3$ and $Z-PPh_3$ species discussed above. As for the latter study, those $Z-P(OPh)_3$ species with Z = main group element show lower d and higher α than the majority of those examples in which Z = transition metal (Spearman rank correlation coefficient[18] = -0.69 significant at better than $>99.99\%$ level). This is in accord with the conclusions of the $Z-PPh_3$ study that P–Z bonding, where Z is an element such as O, N or C, is dominated by σ bonding and that when Z is a transition metal, σ donation is less important and π effects are more important leading to higher d and lower α values. In the $Z-P(OPh)_3$ species studied, the effects of metal oxidation state are less clear cut. Thus species for which $Z = Rh^{III}$ in general have lower d and higher α than those with $Z = Rh^I$ while those fragments with $Z = Fe^{II}$ show less clear differences from those with $Z = Fe^0$. If a more oxidised metal centre acts as a more powerful σ acceptor from, and less effective π donor to the phosphite ligand, such effects would be expected. It is clear that these effects are only part of the story given the rather diffuse nature of the (d, α) distributions, and, for example, the trans influence must play an important role. The geometry of the free triaryl phosphites with known crystal structures all have d and α values that place them at the extreme lower right of the scatterplot in Fig. 3. This contrasts with the $M-PPh_3$ geometries which are distributed approximately symmetrically around the d and α values for PPh_3 itself.[18]

In conclusion, we have shown that in platinum(II) complexes of phosphite **I** the methoxy functionality can influence the chemistry by hydrogen bonding or by co-ordination. We have presented structural evidence supporting the now conventional σ/π-bonding picture for co-ordinated phosphites and have shown that the nature of metal–phosphite bonding can be used to explain the observed tendency of phosphites to be cis in complexes of the type $[PtMe(X)\{P(OR)_3\}_2]$.

Experimental

All preparations were carried out in a dry nitrogen atmosphere using Schlenk techniques. Unless otherwise stated the metal complexes were air stable in the solid state, so once prepared were stored in air. All reaction solvents were dried by refluxing over appropriate drying reagents (calcium hydride for dichloromethane and acetonitrile, sodium–benzophenone for diethyl ether, tetrahydrofuran, toluene, benzene, pentane and hexane, and anhydrous magnesium sulfate for acetone) and distilled under nitrogen prior to use. Commercial reagents were used as supplied and other reagents were prepared by literature methods: [PtCl$_2$(cod)] [20] and [PtMe$_2$(cod)]. [21] Tris(2-methoxyphenyl) phosphite and the platinum(0) complexes were made as previously described. [4] Microanalyses were carried out in the Microanalytical Laboratory of the School of Chemistry, Bristol University. Proton, ^{31}P and [195]Pt NMR spectra were recorded on a JEOL FX90Q or GX400 spectrometer with chemical shifts to high frequency of the references given at the foot of the appropriate tables.

Preparations

cis-[PtCl$_2${P(OC$_6$H$_4$OMe-2)$_3$}$_2$] **1a**. Solid P(OC$_6$H$_4$OMe-2)$_3$ I (4.28 g, 10.7 mmol) was added to a solution of [PtCl$_2$(cod)] (2.00 g, 5.3 mmol) in CH$_2$Cl$_2$ (40 cm^3) to give a colourless solution which was stirred for 30 min. It was then reduced to 4 cm^3 under vacuum followed by dropwise addition of pentane to give the white solid product which was filtered off, washed with pentane (2 × 20 cm^3) and dried *in vacuo* (5.42 g, 96%). The analogous dibromo, diiodo and dimethyl complexes **1b**, **1c** and **7** were made similarly but on a smaller scale (0.2–0.5 mmol) from the appropriate [PtX$_2$(cod)] in 91, 89 and 94% yields respectively.

cis-[PtBr$_2${P(OC$_6$H$_4$OMe-2)$_3$}$_2$] **1b**. A solution of LiBr (0.090 g, 1.02 mmol) was added to a solution of [PtCl$_2${P-(OC$_6$H$_4$OMe-2)$_3$}$_2$] **1a** (0.10 g, 0.090 mmol) in CH$_2$Cl$_2$ (10 cm^3). The resulting mixture was stirred for 2 h to give a yellow solution and then reduced to 5 cm^3 under vacuum. Addition of ethanol (10 cm^3) gave the yellow solid product which was filtered off, washed with water (3 × 10 cm^3), ethanol (10 cm^3) and pentane (3 × 10 cm^3) and dried *in vacuo* (0.11 g, 98%). The iodo complex **1c** was made similarly in 88% yield.

cis-[PtCl(SnCl$_3$){P(OC$_6$H$_4$OMe-2)$_3$}$_2$] **3**. Solid SnCl$_2$ (0.17 g, 0.09 mmol) was added to a solution of [PtCl$_2${P(OC$_6$H$_4$OMe-2)$_3$}$_2$] **1a** (0.10 g, 0.09 mmol) in CH$_2$Cl$_2$ (3 cm^3). The suspension was stirred for 1 h and after this time the solid had dissolved. The solution was then reduced to 0.5 cm^3 under vacuum and the product precipitated by dropwise addition of diethyl ether, filtered off and dried *in vacuo* (0.037 g, 31%). The complex *trans*-[Pt(SnCl$_3$)$_2${P(OC$_6$H$_4$OMe-2)$_3$}$_2$] **4** was made similarly in 92% yield using 2 equivalents of SnCl$_2$.

cis-[PtEt$_2${P(OC$_6$H$_4$OMe-2)$_3$}$_2$] **8**. A solution of AlEt$_3$ in toluene (1.05 cm^3, 1.9 mol dm^{-3}, 2.0 mmol) was added dropwise over 3 min to a solution of [PtCl$_2${P(OC$_6$H$_4$OMe-2)$_3$}$_2$] **1a** (1.0 g, 0.94 mmol) in CH$_2$Cl$_2$ (20 cm^3). The solution changed from colourless to straw to brown and after 1 h water (20 cm^3) was added, followed by more CH$_2$Cl$_2$ (50 cm^3). The organic layer was separated, dried over MgSO$_4$ and then passed down a short Florisil column. The solvent was then reduced to 1 cm^3 and the pale yellow product obtained by dropwise addition of pentane (0.53 g, 54%).

[PtCl(Me){P(OC$_6$H$_4$OMe-2)$_3$}$_2$] **9**. A solution of acetyl chloride in CH$_2$Cl$_2$ (0.14 cm^3, 0.7 mol dm^{-3}, 0.030 mmol) was added dropwise to a vigorously stirred solution of [Pt-

Me$_2${P(OC$_6$H$_4$OMe-2)$_3$}$_2$] **7** (0.10 g, 0.030 mmol) (prepared as above) in CH$_2$Cl$_2$ (20 cm^3) and methanol (5 cm^3). After 1 h the solvent was removed to dryness to leave a white solid which was redissolved in CH$_2$Cl$_2$ and then reprecipitated by dropwise addition of pentane (0.10 g, 97%).

[PtCl(Et){P(OC$_6$H$_4$OMe-2)$_3$}$_2$] **10**. A solution of acetyl chloride in CH$_2$Cl$_2$ (0.047 cm^3, 0.7 mol dm^{-3}, 0.030 mmol) was added to a vigorously stirred solution of [PtEt$_2$ {P(OC$_6$H$_4$OMe-2)$_3$}$_2$] **8** (0.035 g, 0.030 mmol) in CH$_2$Cl$_2$ (3 cm^3) and methanol (0.5 cm^3). After 1 h the solvent was removed to dryness to leave a white solid which was re-dissolved in CH$_2$Cl$_2$ and then reprecipitated by dropwise addition of pentane (0.030 g, 86%). Complex **10** was also prepared in 58% yield using a similar procedure but with [Pt(C$_2$H$_4$){P(OC$_6$H$_4$OMe-2)$_3$}$_2$] replacing [PtEt$_2${P(OC$_6$H$_4$-OMe-2)$_3$}$_2$].

Reactions of HBF$_4$ with [PtMe$_2${P(OC$_6$H$_4$OMe-2)$_3$}$_2$]

85% Ethereal HBF$_4$·OEt$_2$ (0.010 cm^3, 0.06 mmol) was added to a solution of [PtMe$_2${P(OC$_6$H$_4$OMe-2)$_3$}$_2$] (0.05 g, 0.05 mmol) in CD$_2$Cl$_2$ (0.5 cm^3) and the resulting solution examined by ^{31}P NMR spectroscopy at +23 and −80 °C. Three species were identified at low temperatures (see Discussion): **A**, δ 153 [d, [1]*J*(PtP) 3140, [2]*J*(PP) 39], 60.4 [d, [1]*J*(PtP) 8008, [2]*J*(PP) 39]; **B**, δ 130.5 [d, [1]*J*(PtP) 2998, [2]*J*(PP) 39], 65.8 [d, [1]*J*(PtP) 8124, [2]*J*(PP) 39]; **C**, δ 128.5 [d, [1]*J*(PtP) 2852, [2]*J*(PP) 39], 55.1 [d, [1]*J*(PtP) 8008, [2]*J*(PP) 39 Hz]. Using exactly the same procedure but in the presence of water (0.005 cm^3, 0.28 mmol) or MeCN (0.1 cm^3) the product **13** or **14** was identified. The aqua complex **13** was crystallised from CH$_2$Cl$_2$ and pentane.

NMR Studies of the reactions

Of MeI, HCl and Me$_2$CO·HCN with [Pt{P(OC$_6$H$_4$OMe-2)$_3$}$_3$] or [Pt(η^2-C$_2$H$_4$){P(OC$_6$H$_4$OMe-2)$_3$}$_2$]. A solution of the platinum(0) complex (0.05 mmol) in CD$_2$Cl$_2$ (0.35 cm^3) was treated with the reagent (1 equivalent in the case of HCl, 10 equivalents in the cases of MeI and Me$_2$CO·HCN).

Of MeI and Me$_2$CO·HCN with [PtMe$_2${P(OC$_6$H$_4$OMe-2)$_3$}$_2$]. A solution of [PtMe$_2${P(OC$_6$H$_4$OMe-2)$_3$}$_2$] (0.10 g, 0.09 mmol) in CDCl$_3$ (0.4 cm^3) was treated with MeI (0.006 cm^3, 0.09 mmol) or Me$_2$CO·HCN (0.075 cm^3, 0.09 mmol) and the reactions monitored by ^{31}P NMR spectroscopy.

Structure analyses of *cis*-[PtCl$_2${P(OC$_6$H$_4$OMe-2)$_3$}$_2$] **1a** and *cis*-[PtMe(OH$_2$){P(OC$_6$H$_4$OMe-2)$_3$}$_2$]BF$_4$·CH$_2$Cl$_2$ **13**·CH$_2$Cl$_2$

Many of the details of the structure analyses carried out on compounds **1a** and **13**·CH$_2$Cl$_2$ are listed in Table 7. X-Ray diffraction measurements were made at 295 K using Siemens four-circle R3m diffractometers on single crystals mounted in thin-walled glass capillaries with graphite-monochromated Mo-Kα X-radiation (λ = 0.710 73 Å). Cell dimensions for each analysis were determined from the setting angle values of centred reflections.

For each structure analysis, the intensity data were collected for unique portions of reciprocal space and corrected for Lorentz, polarisation, crystal decay and long-term intensity fluctuations, on the basis of the intensities of three check reflections repeatedly measured during data collection. Corrections for X-ray absorption effects were applied on the basis of azimuthal scan data. In the case of complex **1a** data collected for 2θ > 40° were only recorded if a prescan showed intensity > 17.5 counts s^{-1}. The structures were solved by heavy-atom (Patterson and Fourier-difference) methods, and refined by full-matrix least squares against *F*. Except where noted, below all non-hydrogen atoms were assigned anisotropic displacement parameters and refined without positional

Table 7 Details of structure analyses[a] of complexes **1a** and **13·CH$_2$Cl$_2$**

	1a	**13·CH$_2$Cl$_2$**
Formula	C$_{42}$H$_{42}$Cl$_2$O$_{12}$P$_2$Pt	C$_{44}$H$_{49}$BCl$_2$F$_4$O$_{13}$P$_2$Pt
M	1066.7	1200.6
Space group	$P2_1/c$ (no. 14)	$P2_1/n$ (no. 14)
$a/\text{Å}$	11.891(3)	18.834(5)
$b/\text{Å}$	17.153(3)	14.170(4)
$c/\text{Å}$	21.896(7)	20.487(5)
$\beta/°$	101.57(2)	115.39(2)
$U/\text{Å}^3$	4375(2)	4939(3)
$D_c/\text{g cm}^{-3}$	1.62	1.61
$F(000)$	2128	2384
$\mu(\text{Mo-K}\alpha)/\text{cm}^{-1}$	34.9	30.9
Crystal dimensions/mm	0.43 × 0.63 × 0.37	0.20 × 0.26 × 0.16
2θ Range/°	4–50	3–50
Total data	7090	9230
Unique data	6531	8523
Observed data $[F_o^2 > 2\sigma(F_o)^2]$, N_o	5720	3926
Minimum, maximum transmission coefficient	0.090, 0.138	0.206, 0.246
R_{merg}	0.020	0.036
Least-squares variables, N_v	550	424
R	0.028	0.077
R'	0.031	0.074
S	1.04	1.54
g	0.0003	0.0005
Final difference-map features (e Å^{-3})	+0.50, −0.72	+1.3, −1.5

* Details in common: monoclinic; $Z = 4$; ω–2θ scans; scan width ($\omega°$) $1.0 + \Delta_{\alpha_1\alpha_2}$; no multiple-site atoms; $R = \Sigma|\Delta|/\Sigma|F_o|$; $R' = (\Sigma w\Delta^2/\Sigma wF_o^2)^{\ddagger}$; $S = [\Sigma w\Delta^2/(N_o - N_v)]^{\ddagger}$, $\Delta = F_o - F_c$; $w = [\sigma_c^2(F_o) + gF_o^2]^{-1}$, $\sigma_c^2(F_o)$ = variance in F_o due to counting statistics.

Table 8 Atomic coordinates (× 10^4) for complex **1a**

Atom	x	y	z	Atom	x	y	z
Pt	2593(1)	1541(1)	2413(1)	O(52)	500(5)	−675(4)	2874(3)
Cl(1)	1949(2)	2456(1)	1626(1)	C(57)	−723(7)	−836(5)	2776(4)
Cl(2)	2959(2)	2565(1)	3136(1)	O(6)	4438(4)	609(3)	3449(2)
P(1)	2206(2)	611(1)	1712(1)	C(61)	5190(6)	549(5)	3035(4)
P(2)	3099(2)	733(1)	3205(1)	C(66)	5663(7)	1223(5)	2853(4)
O(3)	984(4)	222(3)	1636(2)	C(65)	6465(7)	1156(7)	2462(5)
C(31)	−52(6)	529(5)	1284(3)	C(64)	6772(7)	411(8)	2273(5)
C(36)	−473(7)	193(5)	715(4)	C(63)	6292(7)	−252(6)	2470(4)
C(35)	−1532(8)	462(6)	360(4)	C(62)	5479(6)	−183(5)	2852(4)
C(34)	−2119(7)	1066(6)	603(4)	O(62)	4930(5)	−784(3)	3066(3)
C(33)	−1672(6)	1399(5)	1195(4)	C(67)	5141(7)	−1572(4)	2866(3)
C(32)	−631(6)	1110(5)	1540(4)	O(1)	3028(4)	−109(3)	1897(2)
O(32)	−155(5)	1362(3)	2122(3)	C(11)	2943(7)	−840(4)	1588(3)
C(37)	−567(6)	2080(4)	2330(3)	C(16)	2139(7)	−1372(5)	1707(4)
O(4)	2846(5)	988(3)	3861(2)	C(15)	2112(8)	−2132(5)	1442(4)
C(41)	1768(7)	961(4)	4022(4)	C(14)	2930(9)	−2310(5)	1069(4)
C(46)	765(7)	994(5)	3602(3)	C(13)	3731(8)	−1756(5)	958(4)
C(45)	−288(7)	964(5)	3806(4)	C(12)	3717(7)	−1012(5)	1217(4)
C(44)	−271(8)	918(6)	4444(5)	O(12)	4445(5)	−419(4)	1137(3)
C(43)	786(9)	891(6)	4874(4)	C(17)	5354(7)	−600(5)	802(4)
C(42)	1807(8)	902(5)	4663(4)	O(2)	2234(4)	787(3)	1007(2)
O(42)	2871(6)	856(4)	5026(3)	C(21)	2975(7)	1283(4)	767(3)
C(47)	2943(9)	813(7)	5698(4)	C(26)	4110(7)	1386(5)	1063(4)
O(5)	2521(4)	−99(3)	3075(2)	C(25)	4796(7)	1912(6)	809(5)
C(51)	2295(7)	−623(4)	3518(4)	C(24)	4355(9)	2294(6)	261(5)
C(56)	3120(7)	−830(5)	4039(4)	C(23)	3187(9)	2169(5)	−49(4)
C(55)	2810(8)	−1358(6)	4476(4)	C(22)	2499(8)	1658(5)	215(4)
C(54)	1692(10)	−1643(5)	4375(5)	O(22)	1386(6)	1495(4)	−23(3)
C(53)	843(8)	−1436(5)	3829(4)	C(27)	841(9)	1899(6)	−580(5)
C(52)	1176(7)	−919(5)	3406(4)				

constraints or restraints. The anion and solvent in **13·CH$_2$Cl$_2$** show large anisotropic displacement parameters which may indicate disorder but no satisfactory multisite model was obtained. All hydrogen atoms were constrained to ideal geometries with C–H 0.96 Å and assigned fixed isotropic displacement parameters. No hydrogens were located for the aqua ligands or the solvent molecules in **13·CH$_2$Cl$_2$**.

Final difference syntheses showed no chemically significant features, the largest maxima being close to the metal atoms. Refinements converged smoothly to the residuals given in Table 7. Tables 8 and 9 report the positional parameters for these structure determinations.

Calculations were made with programs of the SHELXTL PLUS[22] package as implemented on a Siemens R3m/V structure-determination system. Complex neutral-atom scattering factors were taken from ref. 23.

Complete atomic coordinates, thermal parameters and bond lengths and angles have been deposited at the Cambridge Crystallographic Data Centre. See Instructions for Authors, *J. Chem. Soc., Dalton Trans.*, 1996, Issue 1.

Table 9 Atomic coordinates (× 10^4) for complex **13·CH$_2$Cl$_2$**

Atom	x	y	z	Atom	x	y	z
Pt	3649(1)	1262(1)	859(1)	C(33)	3341(14)	−2124(17)	744(12)
P(1)	4066(3)	686(4)	1999(3)	C(34)	2650(14)	−2470(17)	756(13)
P(2)	2484(3)	1578(3)	713(3)	C(35)	2397(14)	−2146(17)	1191(12)
O(1)	3851(7)	1375(9)	2497(6)	C(36)	2742(12)	−1381(16)	1656(11)
O(2)	4983(7)	619(9)	2410(6)	O(32)	4393(9)	−921(10)	1210(7)
O(3)	3799(7)	−329(9)	2138(7)	C(37)	4645(16)	−1160(18)	679(15)
O(4)	1756(7)	1416(9)	−50(6)	C(41)	1711(11)	716(14)	−541(10)
O(5)	2243(7)	1043(7)	1261(6)	C(42)	1455(12)	1019(14)	−1273(11)
O(6)	2314(8)	2632(9)	825(7)	C(43)	1446(13)	331(16)	−1768(12)
O(7)	4776(7)	1142(9)	920(6)	C(44)	1606(12)	−537(16)	−1575(12)
C(2)	3386(11)	1776(15)	−159(9)	C(45)	1868(12)	−823(17)	−866(11)
B	6044(47)	3143(36)	954(26)	C(46)	1924(11)	−221(14)	−329(11)
F(1)	6424(20)	2430(21)	1291(20)	O(42)	1303(9)	1958(11)	−1382(8)
F(2)	6118(21)	3381(22)	470(14)	C(47)	1416(16)	2356(17)	−1971(13)
F(3)	5334(12)	2795(16)	797(15)	C(51)	1578(10)	1189(15)	1397(9)
F(4)	6218(13)	3803(16)	1458(10)	C(52)	999(13)	574(16)	1174(11)
C(11)	4100(11)	1250(16)	3264(10)	C(53)	333(14)	673(17)	1357(12)
C(12)	3567(14)	752(16)	3467(13)	C(54)	335(14)	1470(18)	1755(12)
C(13)	3828(16)	673(18)	4220(14)	C(55)	925(15)	2130(20)	1957(13)
C(14)	4508(15)	1053(17)	4643(14)	C(56)	1545(14)	1977(17)	1788(12)
C(15)	4991(14)	1567(16)	4462(12)	O(52)	1066(8)	−170(10)	772(8)
C(16)	4755(12)	1635(14)	3712(11)	C(57)	568(13)	−959(16)	669(13)
O(12)	2916(11)	452(12)	2930(9)	C(61)	2559(11)	3373(13)	520(10)
C(17)	2334(16)	8(19)	3130(16)	C(62)	3317(12)	3785(18)	937(11)
C(21)	5478(12)	−125(15)	2724(11)	C(63)	3565(13)	4520(15)	642(11)
C(22)	6080(12)	−297(15)	2525(11)	C(64)	3078(14)	4802(17)	−35(13)
C(23)	6612(12)	−1003(15)	2871(11)	C(65)	2337(15)	4439(17)	−414(13)
C(24)	6531(14)	−1542(16)	3396(13)	C(66)	2058(13)	3696(17)	−167(11)
C(25)	5963(13)	−1355(17)	3597(12)	O(62)	3693(9)	3391(10)	1622(8)
C(26)	5420(13)	−694(15)	3265(11)	C(67)	4457(14)	3796(22)	2037(13)
O(22)	6069(8)	269(11)	1985(7)	C(99)	5775(17)	5990(29)	1097(17)
C(27)	6729(13)	154(17)	1790(13)	Cl(1)	6633(6)	6652(9)	1655(6)
C(31)	3412(12)	−1030(15)	1615(10)	Cl(2)	5138(6)	6336(9)	1549(5)
C(32)	3712(11)	−1348(16)	1160(10)				

References

1 Du Pont, U.S. Pat., 3 766 237, 1973; C. A. Tolman, R. J. McKinney, W. C. Seidel, J. D. Druline and W. R. Stevens, Adv. Catal., 1985, 33, 1 and refs. therein.

2 Union Carbide, U.S. Pat., 4 668 651, 1987; 4 769 498, 1988; 911 518, 1992; Eur. Pat., 577 042, 1994; BASF, World Pat., 525, 1995.

3 N. Sakai, S. Mano, K. Nozaki and H. Takaya, J. Am. Chem. Soc., 1993, 115, 7033; G. D. Cuny and S. L. Buchwald, J. Am. Chem. Soc., 1993, 115, 2066; T. J. Kwok and D. J. Wink, Organometallics, 1993, 12, 1954; N. Greene, H. Taylor, T. P. Kee and M. Thornton-Pett, J. Chem. Soc., Dalton Trans., 1993, 821; S. N. Poelsma and P. M. Maitlis, J. Organomet. Chem., 1993, 451, C15; A. Trzeciak and J. J. Ziólkowski, J. Organomet. Chem., 1994, 464, 107; P. W. N. M. van Leeuwen, G. J. H. Buisman, A. van Rooy and P. C. J. Kamer, Recl. Trav. Chim., 1994, 61; N. Sakai, K. Nozaki and H. Takaya, J. Chem. Soc., Chem. Commun., 1994, 395; B. Moasser, C. Gross and W. L. Gladfelter, J. Organomet. Chem., 1994, 471, 201; G. J. H. Buisman, E. J. Vos, P. C. J. Kamer and P. W. N. M. van Leeuwen, J. Chem. Soc., Dalton Trans., 1995, 409; A. van Rooy, E. N. Orij, P. C. J. Kamer and P. W. N. M. van Leeuwen, Organometallics, 1995, 14, 34; A. van Rooy, P. C. J. Kamer, P. W. N. M. van Leeuwen, N. Veldman and A. L. Spek, J. Organomet. Chem., 1995, 494, C15; B. M. Trost, J. R. Parquette and A. L. Marquart, J. Am. Chem. Soc., 1995, 117, 3284.

4 M. J. Baker, K. N. Harrison, A. G. Orpen and P. G. Pringle, J. Chem. Soc., Dalton Trans., 1992, 2607 and refs. therein.

5 M. J. Baker, K. N. Harrison, A. G. Orpen, P. G. Pringle and G. S. Shaw, J. Chem. Soc., Chem. Commun., 1991, 803; M. J. Baker and P. G. Pringle, J. Chem. Soc., Chem. Commun., 1991, 1292; 1993, 314.

6 E. Lindner and A. Bader, Coord. Chem. Rev., 1991, 108, 27 and refs. therein.

7 N. Ahmad, E. Ainscough, T. A. Janas and S. D. Robinson, J. Chem. Soc., Dalton Trans., 1973, 1148.

8 P. S. Pregosin and S. N. Sze, Helv. Chim. Acta, 1978, 61, 1848; P. S. Pregosin, A. Albinati and H. Ruegger, Inorg. Chem., 1984, 23, 3223; A. Pidcock, P. B. Hitchcock and G. Butler, J. Organomet. Chem., 1979, 181, 47.

9 J. F. Almeida, H. Azizian, C. Eaborn and A. Pidcock, J. Organomet. Chem., 1989, 362, C21; A. R. Siedle, G. Filopovich, P. E. Toren, F. J. Palensky, R. A. Newmark, R. W. Duerst, W. L. Stebbings, H. E. Mishmash, K. Melancon and D. A. Bohling, Inorg. Chem., 1985, 24, 2216; A. Pidcock, C. Eaborn and K. Kunda, J. Chem. Soc., Dalton Trans., 1981, 933.

10 W. R. Meyer and L. M. Venanzi, Angew. Chem., Int. Ed. Engl., 1984, 23, 529.

11 T. M. Gomes-Carneiro, R. D. Jackson, J. H. Downing, A. G. Orpen and P. G. Pringle, J. Chem. Soc., Chem. Commun., 1991, 317.

12 K. N. Harrison, Ph.D. Thesis, Bristol University, 1990.

13 F. H. Allen and A. Pidcock, J. Chem. Soc. A, 1968, 2700; J. A. Davies and F. R. Hartley, Chem. Rev., 1981, 81, 79.

14 D. G. Gilheany, Chem. Rev., 1994, 94, 1339.

15 R. J. McKinney and C. Roe, J. Am. Chem. Soc., 1986, 108, 5167 and refs. therein.

16 A. N. Caldwell, L. M. Muir and K. W. Muir, J. Chem. Soc., Dalton Trans., 1977, 2265.

17 W. Hummel, K. Huml and H.-B. Bürgi, Helv. Chim. Acta, 1988, 71, 1291.

18 B. J. Dunne, R. B. Morris and A. G. Orpen, J. Chem. Soc., Dalton Trans., 1991, 653.

19 F. H. Allen, O. Kennard and R. Taylor, Acc. Chem. Res., 1983, 16, 146.

20 J. X. McDermott, J. F. White and G. M. Whitesides, J. Am. Chem. Soc., 1976, 98, 6521.

21 E. Costa, M. Ravetz and P. G. Pringle, Inorg. Synth., 1996, 31, in the press.

22 G. M. Sheldrick, SHELXTL PLUS, Revision 4.2, University of Göttingen, 1990.

23 International Tables for X-Ray Crystallography, Kynoch Press, Birmingham, 1974, vol. 4.